REPORT DOCUMENTATION PAGE

Form Approved
OMB No. 0704-0188

1. AGENCY USE ONLY (Leave blank)	2. REPORT DATE	3. REPORT TYPE AND DATES COVERED
	April 28, 1995	

4. TITLE AND SUBTITLE

Conformal Temperature Sensors from Ion-Implanted Polymers

5. FUNDING NUMBERS

DAAL03-92-C-0017

6. AUTHOR(S)

Mary G. Moss (1), James Kaufmann (1),
Ryan E. Giedd (2), Yongqiang Wang (2)

7. PERFORMING ORGANIZATION NAME(S) AND ADDRESS(ES)

(1)Brewer Science, P. O. Box GG, Rolla, MO 6540
(2) Southwest Missouri State University
901 S. National Ave., Springfield, MO 65804

8. PERFORMING ORGANIZATION REPORT NUMBER

9. SPONSORING / MONITORING AGENCY NAME(S) AND ADDRESS(ES)

U.S. Army Research Office
P.O. Box 12211
Research Triangle Park, NC 27709-2211

10. SPONSORING / MONITORING AGENCY REPORT NUMBER

ARO 30359.3-EL-SB2

11. SUPPLEMENTARY NOTES

The views, opinions and/or findings contained in this report are those of the author(s) and should not be construed as an official Department of the Army position, policy, or decision, unless so designated by other documentation.

12a. DISTRIBUTION / AVAILABILITY STATEMENT

Approved for public release; distribution unlimited.

12b. DISTRIBUTION CODE

13. ABSTRACT *(Maximum 200 words)*

Previous work demonstrated the feasibility of forming thin-film, negative temperature coefficient, temperature sensors from ion implanted polymer films. Semiconductive films of ion implanted polymers have the advantage that they can be applied to a variety of substrates, including flexible plastic, and patterned by conventional lithographic processes. One major advantage is their high degree of solvent and abrasion resistance. During Phase II, polymer and processing conditions which resulted in stable films were identified. Several types of devices were demonstrated: temperature sensors with 10-50 micrometer geometries, an IC incorporating an implanted thermistor as protection from overheating, and a temperature sensing array for measuring thermal gradients. Phase II results demonstrated that these materials have wide-ranging uses in the semiconductor industry for temperature sensing and applications based on resistance-temperature variations, such as vacuum measurement and bolometry.

14. SUBJECT TERMS	15. NUMBER OF PAGES
temperature sensors, thermistors, microsensors, conductive polymers, ion implanted polymers	16. PRICE CODE

17. SECURITY CLASSIFICATION OF REPORT	18. SECURITY CLASSIFICATION OF THIS PAGE	19. SECURITY CLASSIFICATION OF ABSTRACT	20. LIMITATION OF ABSTRACT
UNCLASSIFIED	UNCLASSIFIED	UNCLASSIFIED	UL

Table of Contents

List of Appendices, Illustrations, and Tables

1.0 Statement of Problem Studied

The rapid growth of the sensors industry, and in particular, miniaturized sensors, has created needs for new types of materials with unique properties and processing capabilities. Conducting polymers have been proposed for many types of sensor applications, but their use in real devices has been limited by instability and processing difficulties.

During the Phase I SBIR contract, "Development of Miniature Temperature Sensors," Brewer Science, Inc., and Southwest Missouri State University demonstrated the feasibility of forming thin-film, negative temperature coefficient, temperature sensors from nitrile-containing polymers which were made conductive by ion implantation.[1] The temperature sensors have the advantage that they can be coated from solution directly onto the surface to be measured, they can be lithographically patterned without loss of conductivity, and they are extremely solvent- and abrasion-resistant.

As this work was extended into Phase II, the goals were to demonstrate three types of prototype devices: miniature sensors to be used in microelectronics circuits, an active sensor for protecting ICs from overheating, and a temperature sensing array for measuring thermal gradients. Phase II performance objectives included developing the process to achieve controllable resistance-temperature characteristics with a maximum use temperature of 100°C and a stability of 0.05°C/year.

The basic materials work which was performed in the course of Phase II indicated that the materials have much more wide-ranging commercial applications than temperature sensors. Ion implanted polymer films could be used in miniature pirani vacuum gauges, microbolometers, and other applications. Demonstrations of these applications were made and appropriate patents were filed. This report provides a short summary of each area of work studied during Phase II. When the technical details are considered to be trade secret, the descriptions are abbreviated.

2.0 Experimental Techniques

The basic process involved spin coating the precursor polymer onto a flat substrate (glass microscope slides, 7059 glass pieces, or silicon wafers) and baking to remove solvent. Film thicknesses tested ranged from 500 angstroms to 26 micrometers; the preferred film thickness was less than or equal to twice the mean range of ions in the film. Conductivity was induced in the polymer by ion implantation with parameters from Table 1. Implantation to 50 keV was

performed by Southwest Missouri State University; higher energy implantation was performed by UES, Inc., Dayton, Ohio.

Table 1
Implantation parameters

Film thickness	500 angstroms to 26 micrometers
Ion energy	25-175 keV
Ion type	$^{11}B^+$, $^{28}N_2^+$, $^{14}N^+$, $^{49}BF_2^+$, $^{19}F^+$, $^{75}As^+$
Fluence	$1x10^{15}$ ions/cm^2 to $1x10^{17}$ ions/cm^2
Current density	0.5 microamps/cm^2 to 2 microamps/cm^2
Resistance range	200 ohms/square to 1 gigohm/square

A variety of precursor polymers were tested. Polystyrene, polymethyl methacrylate, polysulfone, poly(acrylonitrile-co-methyl methacrylate((93/7), benzocyclobutene resins, and poly(styrene-co-acrylonitrile)(55/45) were purchased and used as supplied. Poly(styrene-co-methacrylonitrile) copolymers (54/46, 28/72, and 69/31 molar ratios) were synthesized by free radical polymerization and their compositions were determined by elemental analysis. Polyimide precursors, including PMDA/ODA polyimides (pyromellitic dianhydride/oxydianiline), BTDA/ODA polyimide (benzophenone tetracarboxylic dianhydride/ oxydianiline), and BTDA-4APS polyimide (benzophenone tetracarboxylic dianhydride/ 4-aminophenyl sulfone), were synthesized by the reaction of the appropriate dianhydride and diamine in N-methylpyrrolidone solvent.

While a variety of polymer types and implantation conditions were tested, a majority of work was performed with optimized conditions which included polystyrene-acrylonitrile films implanted with 50 keV N^+ ions to a fluence of $5x10^{16}$ ions/cm^2 or $1x10^{17}$ ions/cm^2. These conditions produced films with resistivity in the range of 7 to 9 megohms/square.

For high resistance samples, gold electrodes were evaporated onto the films through a mask to form electrical contact for a two-probe conductivity measurement. Contact resistance was shown to be negligible in these cases. For samples with resistivity lower than 100 kilohms per square, resistivity was measured with a four point probe.

Lithographically patterned samples were prepared by spinning, coating, and baking the polymer onto silicon dioxide wafers which had been previously patterned with gold electrodes. After implantation, the conducting film was patterned by oxygen RIE etching through a positive

photoresist etch mask. The electrical configuration was a 16-element resistor matrix with a common bus line. The wafer was diced and resistor matrices were bonded and packaged into dual in-line packages. When testing required exposure to the atmosphere, lids were omitted from the packages.

Resistance-temperature measurements from room temperature to 30 K were made at Southwest Missouri State University. Samples of implanted films on 1" by 3" glass substrates with evaporated gold connections were cooled in a refrigerated chamber containing helium gas. Resistance was measured continuously with a Keithley electrometer using a constant voltage method. Temperature was measured simultaneously with a platinum RTD with a 2 K systematic error and reproducibility of 0.02 Kelvin. Sample resistance was measurable within 5% due to temperature control.

Resistance-temperature measurements at temperatures higher than 25°C were made at Brewer Science by regulating the temperature with a thermally controlled chuck and measuring the temperature with a thin film temperature sensor. Resistance was measured with a Keithley electrometer through a computer interface.

Thermal stability tests were also performed by heating the samples in a Blue M oven. Sample temperature was measured with a thermocouple, and the resistance was measured simultaneously.

3.0 Ambient resistance; uniformity and stability

3.1 25°C resistance

The resistance at 25°C was a strong function of polymer type, fluence, ion, and ion energy. Resistances representative of various sample conditions ranged from insulating to 200 ohms/square. The 25°C resistance was strongly correlated to the decrease of film thickness after implantation, corresponding to densification and carbonization of the film.

Out of 500 patterned and packaged resistors which were prepared according to the standard conditions specified in section 2.0, the 1σ deviation in bulk resistivity was 1.88%. The majority of variation could be attributed to thermal changes during measurement.

3.2 Ambient stability

At the end of Phase I, drift of resistance as a function of time at room temperature was seen. The total resistance shift amounted to 0.5% in every 100 hours of measurement. A

major objective of Phase II work was to eliminate this ambient resistance drift.

Ambient resistance testing was performed on unpassivated samples with a size of approximately 1 cm^2. Electrical contact was made by evaporation of gold leads to the top of the implanted film. Temperature of the sample was maintained to 25°C$\pm$ 0.5°C.

The fluence, the film thickness, and the polymer type had the most influence on the aging rate of the film. Increasing the fluence, even by an order of magnitude beyond a certain critical fluence, did not result in a decrease in aging rate even through the resistance continued to decrease. The stability and resistance, ultimately, were most sensitive to film thickness and polymer type. The optimum conditions were identified above. Still, the films exhibited ambient resistance changes of 0.1%/100 hour period.

Thermally annealing the films was effective in stabilizing the resistance. Films which had been implanted to the optimum conditions and annealed had a stability within measurement error (<0.1°C for 1 year).

3.3 Electrical stability to breakdown

A small geometry resistor with dimensions 40µm wide by 10µm long was biased with 90 volts (a field of 90,000 V/cm) and the current monitored for about 50 minutes. The range of the current was from 50.85 to 51.01 µAmps (a variation of 0.006 Mohms, about 0.3%) possibly accountable by variations in room temperature (the sample was not temperature controlled). Three hours after the test, the measured resistance was within about one percent of the initial resistance before the test.

Resistors with geometries of 20 to 50 µm, and die bonded in DIP chips without lids, were subjected to successively higher voltages until the polymer component failed. Resistors withstood electric fields up to 40,000 volts/cm.

3.4 Solvent and abrasion resistance

A major advantage of the implanted films was their high degree of chemical and abrasive resistance. Standard samples could be soaked in propylene glycol monomethylether acetate, a strong solvent for unimplanted polymer, for 18 hours without change in conductivity or appearance. Likewise, patterned resistors could be exposed to buffered oxide etchant, photoresist developer, aqua regia, chrome etchant, and various organic solvents without change of conductivity.

Films which were thinner than twice the mean range of ions also had a hardness greater than silicon, (a Mohs scale hardness of 7.0.) Thicker films could be scratched due to the underlying, unimplanted portion of the film.

4.0 Resistance-temperature characteristics; relation to conduction mechanisms

4.1 Conduction mechanisms; depth dependence of conductivity

The results of this investigation have been published in reference 2, and are only summarized here. Figure 1 shows a typical resistance-temperature curve of an implanted polymer film.

The resistance-temperature characteristics of implanted films were measured from 30K to 298K as previously described. The data were modeled according to variable-range hopping mechanisms of conductivity as described by Mott.[3,4] The method of modeling is described in reference 5. The conductivity mechanism was a combination of one-dimensional and three-dimensional variable-range hopping (VRH). Analysis of various fluences and energies of implantation had previously shown that the more heavily implanted films had a greater degree of 3d hopping.[5]

Ion trajectories can be calculated using the Trajectory and Range of Ions in Matter (TRIM) code.[6] Calculations predict a teardrop-shaped distribution of damage in the film due to nuclear stopping. Electronic stopping peaks near the surface. Presumably, the depth profile of conductivity in the film would be related to the damage distribution, in that the layers receiving the implant damage which causes conductivity would have a more conductive, 3d component, whereas the areas receiving damage which results in less conductive material would have a greater portion of 1d hopping.

To test this theory, unpatterned, implanted films of poly styrene-co-acrylonitrile (50 keV N^+; fluences of $5x10^{16}$ ions/cm^2 and $1x10^{17}$ ions/cm^2) were etched using oxygen plasma to selectively remove layers of the film. Remaining thicknesses were measured with a profilometer. The resistivity as a function of temperature was measured as a function of remaining thickness for each layer of the film, and was modeled according to Mott's hopping theories to determine the one-and three- dimensional contributions. The results showed that the layers that were close to the surface had higher conductivity (Figure 2) and a higher degree of 3-dimensional VRH mechanism; toward the deeper regions of the film, near the mean range of the implant ion (1500Å), 1d-VRH dominated.[2] These results suggested that the implant damage

leading to the majority of the conductivity was due to the electronic stopping contribution. The ambient resistance instability of the unannealed films appeared to be related to the 1d hopping portion of the conductivity.

Table 2
Beta values, selected samples
Poly(styrene-co-acrylonitrile)

Ion (energy)	Fluence ions/cm^2	$(T-T_O)$,K	β	$\alpha(T_O)$
N^+ (50 keV)	$5x10^{15}$	200-300	2430	-2.7%/°C
N^+ (50 keV)	$5x10^{15}$	100-150	1250	-5.6%/°C
N^+ (50 keV)	$1x10^{16}$	200-300	1760	-2.0%/°C
N^+ (50 keV)	$1x10^{16}$	100-150	1090	-4.8%/°C
N^+ (50 keV)	$5x10^{16}$	200-300	1710	-1.9%/°C
N^+ (50 keV)	$5x10^{16}$	100-150	976	-4.3%/°C
N^+ (50 keV)	$1x10^{17}$	200-300	1580	-1.8%/°C
N^+ (50 keV)	$1x10^{17}$	100-150	1010	-4.5%/°C

4.2 Dependence of R/T characteristics on implantation parameters

Throughout the entire measured range, the R/T curve could be fit to an equation which showed the combined effect of 1D and 3D variable range hopping:

$$\rho(T) = \rho_{1D}(T) + \rho_{3D}(T)$$
$$= \rho_1(T) \exp (T_1/T)^{1/2} + \rho_3(T) \exp(T_3/T)^{1/4}$$

where $\rho_1(T)$ and $\rho_3(T)$ are the 1D and 3D VRH components, and T_1 and T_3 are constants.

Over short temperature ranges, the fit to a standard thermistor R-T equation permitted the calculation of thermistor beta values,

$$\ln R = A + \beta/T,$$

where the temperature coefficient of resistance (TCR) is defined as

$$\alpha = -\beta/T^2.$$

Table 2 shows several examples of implantation conditions, thermistor beta values, and TCRs over short temperature ranges. In general, the higher the resistivity, the greater the slope of the RT curve, a phenomenon which is characteristic of other semiconductors.

The R-T curve from 100 K to 300 K was retraceable over a time period of a year within the measurement precision. The curve below 100 K had greater variability, possibly due to temperature control and measurement of the high resistances.

5.0 Compositional analysis of implanted films

In order to determine the microstructure of the above polymer layers to correlate the amount of film damage with the conductivity, the etched samples were analyzed by Elastic Recoil Detection (ERD) to determine carbon and hydrogen elemental composition of implanted films.[7] Hydrogen composition was calculated as the total hydrogen content in atoms/cm^2 divided by the film thickness after implantation. ERD experiments were conducted on an Ionex 2x1.7 MV Tandem Accelerator in the Ion Beam Laboratory at the University of Michigan.

The pristine polymer contained a relative atomic ratio of carbon to hydrogen of 50/50. Implantation caused hydrogen loss which was accompanied by thickness loss of up to 50%. The thickness loss was directly correlated to the conductivity as well as the fluence.

Several sets of samples were analyzed:

1) Varying thickness samples: Films from 500 to 5000 Å, implanted to a dose of $5x10^{16}$ ions/cm^2. In these samples, the hydrogen distribution was shown to be nonuniform within the implanted layer, and the major hydrogen depletion occurred in a shallow surface layer.

2) Etched samples: as prepared in section 4.1, above.

Figure 3 shows the relative hydrogen content as a function of depth below the surface for the etched layers. The major hydrogen depletion occurred in the shallow surface layer, which was consistent with the results of the varying-thickness experiments.

3) Varying-dose implanted samples: Original thickness of 2000 Å, implanted to a dose range of $5x10^{15}$ ions/cm^2 to $5x10^{17}$ ions/cm^2. The higher the dose, the greater the amount of hydrogen loss. For a film implanted with $5x10^{17}$ ions/cm^2, only 7.6% hydrogen remained in the film.

The results of compositional analysis were consistent with R/T analysis, which showed higher conductivity and more 3D hopping at the surface.

6.0 Thermal stability

6.1 Thermal cycling, 25°C to 100°C

Thermal cycling experiments were conducted on two types of samples: those prepared on 1"x3" glass substrates, and patterned resistors on a silicon wafer with the configuration shown in Figure 4.

The resistance-temperature response had a hysteresis in the 25° return value of the resistance on the first cycle. Subsequent cycles were retraceable within 0.2%, which was within temperature control accuracy. The drop in 25°C resistances ranged from approximately 1% to 20% for the many different conditions and polymers that were tested.

The percent change was strongly related to the polymer type and the implantation conditions. Films with lower resistance had less resistance change after the first cycle. A plot of sample resistance versus per cent change in the return cycle is shown in Figure 5. Likewise, the percent drop in resistance after the first cycle was related to the maximum temperature which the films encountered.

Long-term heating (700 hours) at 100° caused 15% change in the 25° resistance.

6.2 Thermal stability to 250°C

Resistances was monitored while the samples were heated to 250°C in air in an oven. Upon reaching the temperature of 250°C, the temperature was maintained for 60 minutes while resistance was measured.

Using the resistance-temperature behavior of each sample which was determined during the heat up cycle, an equivalent error in temperature reading from the beginning of the 250°C hold to the end of the hold was calculated. These errors ranged from 70°C (BTDA/ODA polyimide) to <1°C (polystyrene-acrylonitrile) and 5°C for polystyrene.

Similar experiments were conducted at a temperature of 120°C for a heating period of 30 minutes. In this case, the

results were analyzed as a percent change in resistance at that temperature. The percentage change in resistance from the beginning to the end of the heating cycle ranged from 25% for BTDA/ODA polyimide to 0.5% for polystyrene.

Clearly, the thermal stability of the implanted film was directly related to polymer type. Surprisingly, the thermal stability of the original, unimplanted polymer had little correlation with the thermal stability of the resistance of the implanted film. Softer polymers with lower Tg and lower thermal stability in the unimplanted form, had greater thermal stability of the resistance in the implanted, conductive form. Polyimides had especially poor thermal stability of the resistance; styrene-acrylonitrile blends were particularly stable.

7.0 Commercial applications of the technology

7.1 Thin film contact temperature sensor for surface temperature measurement

A four-inch silicon wafer was patterned with 13 ion implanted thermistors as shown in Figure 4. The wafer was placed on a temperature controlled chuck and cycled slowly from 25°C to 100°C twice with 15 minute holds at 25° and 100°. The resistances of the sensors was measured with small diameter conductive foam strips to reduce thermal loading. Resistances ranged from 4 Mohms at 25°C to 0.8 Mohms at 100°C. The wafer temperature was monitored with a thin film temperature sensor. The ion implanted temperature sensors were read non-sequentially through a computer controlled relay bank. The collected data was analyzed to obtain a response curve for each resistor and the calculated temperature variations were plotted. The temperature variations were as expected--several degrees hotter in the center of the chuck than at the edges. A hotspot on the chuck at 100°C was indicated to be about 1 cm off the center of the chuck. The temperature resolution for this initial testing was about 0.5°C.

7.2 Thermal overload protective circuit

The ability to protect a vital component of a circuit from overheating by monitoring the temperature, and shutting off the component when the temperature reaches a certain limit, was demonstrated using implanted thermistors deposited directly on the outside of the package. This technology could be used to deposit thermistors directly onto sensitive areas of an integrated circuit to replace thermocouples which are attached to individual components.

The dual in-line (DIP) package protection feature of ion implanted polymers is demonstrated by the circuits shown in

Figures 6a and 6b. The purpose of these circuits is to deliberately overheat the amplifier U1 by overloading the output. This overload condition is accomplished by toggling the switch, S1. The oscillator, U2, provides the test signal visible as a flashing light at D2. In normal operating conditions, S1 open, the amplifier with the protection package, U1, will cause the oscillator indicator, D2, to flash. The power for U1 is derived from the circuit shown in Figure 6a. Under normal conditions, the package temperature sensor, R1, is at a relatively high resistance. At this high resistance, the power to U1 can be controlled by the temperature set point control, VR1. By moving VR1 counterclockwise, the temperature at which power will be removed from U1 increases. Thus, VR1 can be set so that under normal operating conditions, power is applied to U1, so that lights D3 and D4 are on, and the final output indicator, D1 flashes. Closing S2 provides an overload condition for U1. As a result, U1 heats, and the package protection resistor, R1, decreases in resistance. This causes a change in the voltage with respect to the VR1 set point, resulting in a cut off of power for U1 through the relay RL1. This turns off U1, D3, and D4, and since U1 is off, the flashing light, D1, turns off. Since the power is off to U1, the package cools and the circuit reapplies power to U1. If the overload is still present, the circuit will turn off U1 again after a few seconds. If the overload is not present the output will continue to oscillate. In this way, the ion implanted package prevents any harm to U1. Without the protection package, U1 would overheat and fail in 10 minutes.

7.3 Other applications

The ability to pattern small geometry elements with a high resistance-temperature response suggests several other applications which were explored to various extents during Phase II.

One such application is infrared sensing (bolometry). We have shown that the resistors can be released from the substrate in the middle to form suspended films with some degree of thermal isolation from the substrate.[8] The ability to detect infrared radiation was demonstrated during Phase II, although the sensitivity and response time were not quantified.

Another type of device based on the R-T properties of the material is air flow or vacuum sensing. Suspended ion implanted polymer bridges which were developed under NSF grant III-9362010,[8] can be used to make pirani-type vacuum gauges. These gauges respond to pressure in the range of 760 to 1 torr, at which point the mean free path of the gas molecules becomes the same magnitude as the dimensions of the device (20 micrometers length, 30 micrometers width.) The

same technology is expected to be applicable to the fabrication of anemometers for the measurement of gas flow.

A microprocessor-controlled circuit was built which displayed the pressure according to a previously stored resistance-temperature calibration curve.[9] This control circuitry could be used to display temperature rather than pressure, if desired for other applications.

8. Summary

During Phase II, polymer and processing conditions which resulted in stable films were identified. A strong correlation between stability and polymer type was demonstrated.

Semiconductive films of ion implanted polymers have the advantage that they can be applied to a variety of substrates, including flexible plastic, and patterned by conventional lithographic processes. One major advantage which is unique among other types of conductive polymers is their high degree of solvent and abrasion resistance. Their uses are wide-ranging in the semiconductor industry for temperature sensing and applications based on resistance-temperature variations, such as vacuum measurement and bolometry. Phase II work resulted in several patents on these applications. Brewer Science is currently researching the market for each of these applications, in order to determine the best route to commercialization.

9. List of publications and technical reports

R. E. Giedd, D. Robey, Y. Q. Wang, M. G. Moss, and J. Kaufmann, "The Electronic Microstructure in the Implant Layer of Ion Implanted Polymers," Mat. Res. Soc. Symp. Proc., Vol. 316, p. 75 (1994).

Y. Q. Wang and R. E. Giedd, "Compositional Analysis in Ion Implanted Polymers," to be submitted.

Y. Q. Wang, R. E. Giedd, M. G. Moss, and J. Kaufmann, "Ion Implanted Polymers as Smart Materials," presented at the 13th International Conference on the Application of Accelerators in Research and Industry, Nov. 7-10, 1994.

Y. Q. Wang, R. E. Giedd, J. Kaufmann, "Investigation of Polymer Microbridge Resistors as Pirani Pressure Sensors," to be submitted.

Interim progress reports: 7 JUL 92- 31 DEC 92, 1 JAN 93- 30 JUN 93, 1 JAN 93- 31 DEC 93, 1 JUL 94- 31 DEC 94.

10. List of participating scientific personnel showing advanced degrees

Brewer Science personnel:
Mary G. Moss
James Kaufmann
Shawn Sitton
Koby Smith
Terry Toddy

SMSU personnel:
Ryan Giedd
Yongqiang Wang
David Robey

11. Report of inventions

"Method for Making Electrical Devices from Ion-Implanted Conductive Polymers," Application number 08/342/865, filed November 21, 1994.

"Pirani Pressure Sensor," filed February 7, 1995; application number 08/384,826.

"Conductive Polymer-based Microbolometer," to be filed in 1995.

Fourth application which proprietary at this time.

12.0 Bibliography

1. M. Moss, et al., "Development of Miniature Temperature Sensors," final report for contract no. DAAL03-90-C-0012, 1991.

2. R. E. Giedd, D. Robey, Y. Q. Wang, M. G. Moss, and J. Kaufmann, "The Electronic Microstructure in the Implant Layer of Ion Implanted Polymers," Mat. Res. Soc. Symp. Proc., Vol. 316, p. 75 (1994).

3. N. F. Mott, Philo. Mag., 19, p.835 (1969).

4. N. F. Mott and E. A. Davis, Electronic Processes in Non-Crystalline Materials (Clarendon Press, Oxford, UK, 1979).

5. Yongqiang Wang, S. S. Mohite, L. B. Bridwell, R. E. Giedd, C. J. Sofield, "Modification of high temperature and high performance polymers by ion implantation," J. Materials Research, vol. 8, no. 2, p. 1 (1993).

6. J. F. Ziegler, J. P. Biersack, and U. Littmark, The Stopping and Range of Ions in Solids, Pergamon Press, Oxford, 1985.

7. Y. Q. Wang and R. E. Giedd, "Compositional Analysis in Ion Implanted Polymers," to be submitted.

8. M. G. Moss, J. Kaufmann, Y. Q. Wang, D. S. Robey, R. E. Giedd, "Polymer-Based Piezoresistive Sensors," final report for NSF grant III-9362010, November 11, 1994.

9. Y. Q. Wang, R. E. Giedd, J. Kaufmann, "Investigation of Polymer Microbridge Resistors as Pirani Pressure Sensors," to be submitted.

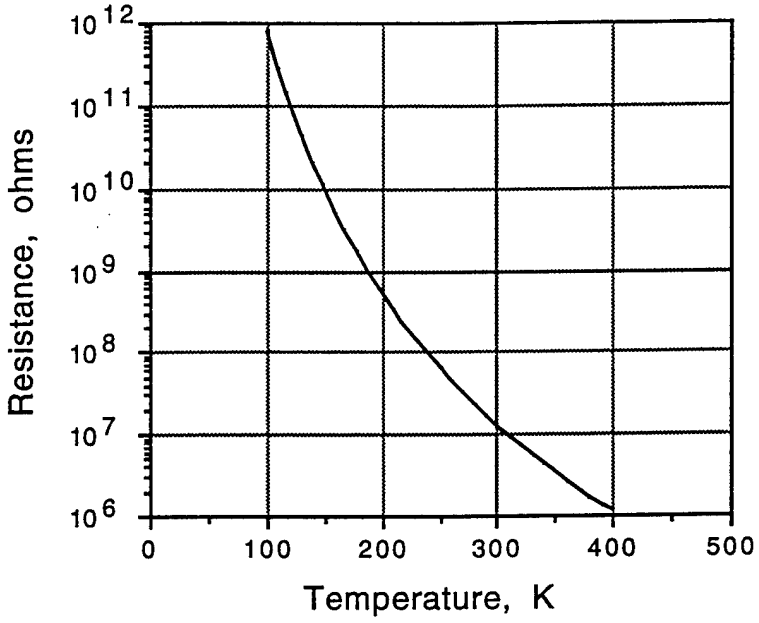

Figure 1: RT curve of 2000Å thick implanted poly(styrene-acrylonitrile) (PSA). Conditions of implantation are: Ion, 50 keV $^{14}N^{+}$: Fluence, $5x10^{16}$ ions/cm^2.

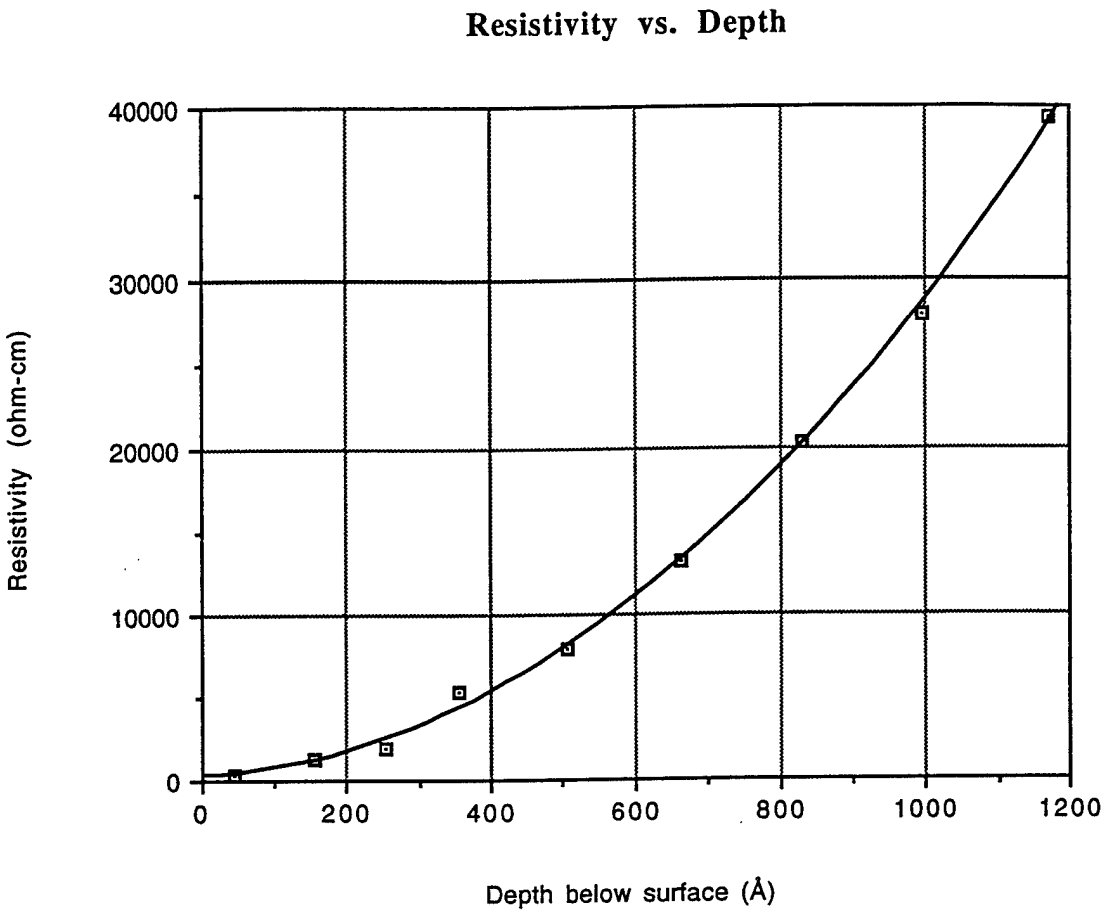

Figure 2: Depth dependence of the conductivity of a 5000Å thick (before implantation) implanted poly(styrene-acrylonitrile) film. Conditions of implantation are: Ion, 50 keV $^{14}N^{+}$: Fluence, $1x10^{17}$ ions/cm^2.

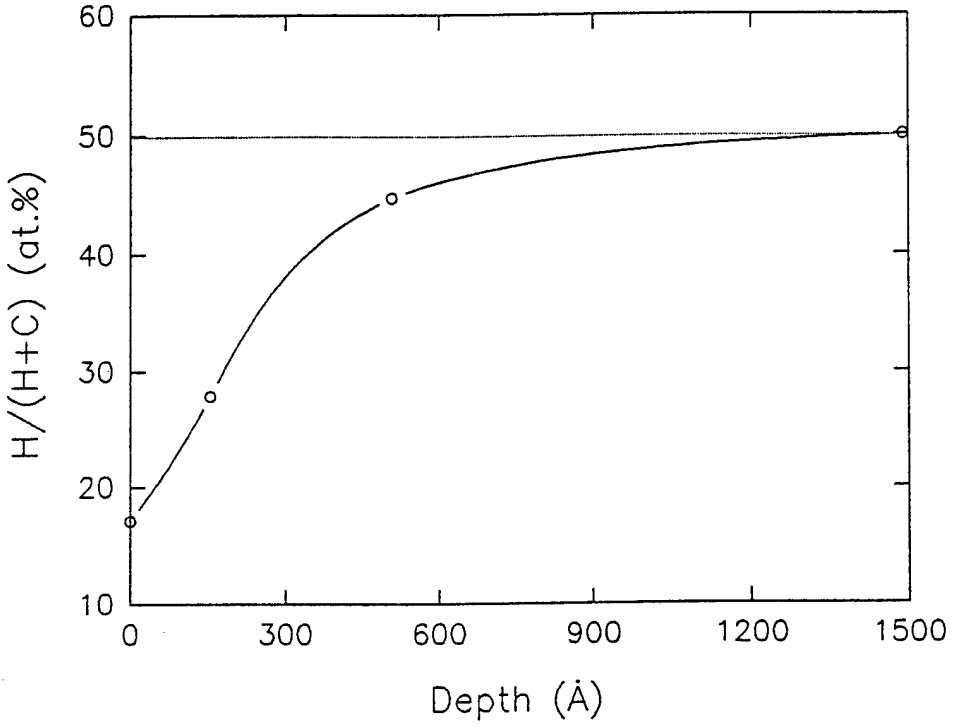

Figure 3: Depth dependence of the hydrogen atomic composition in a 5000Å thick (before implantation) implanted poly(styrene-acrylonitrile) film. Conditions of implantation are: Ion, 50 keV $^{14}N^{+}$: Fluence, $5x10^{16}$ ions/cm^2.

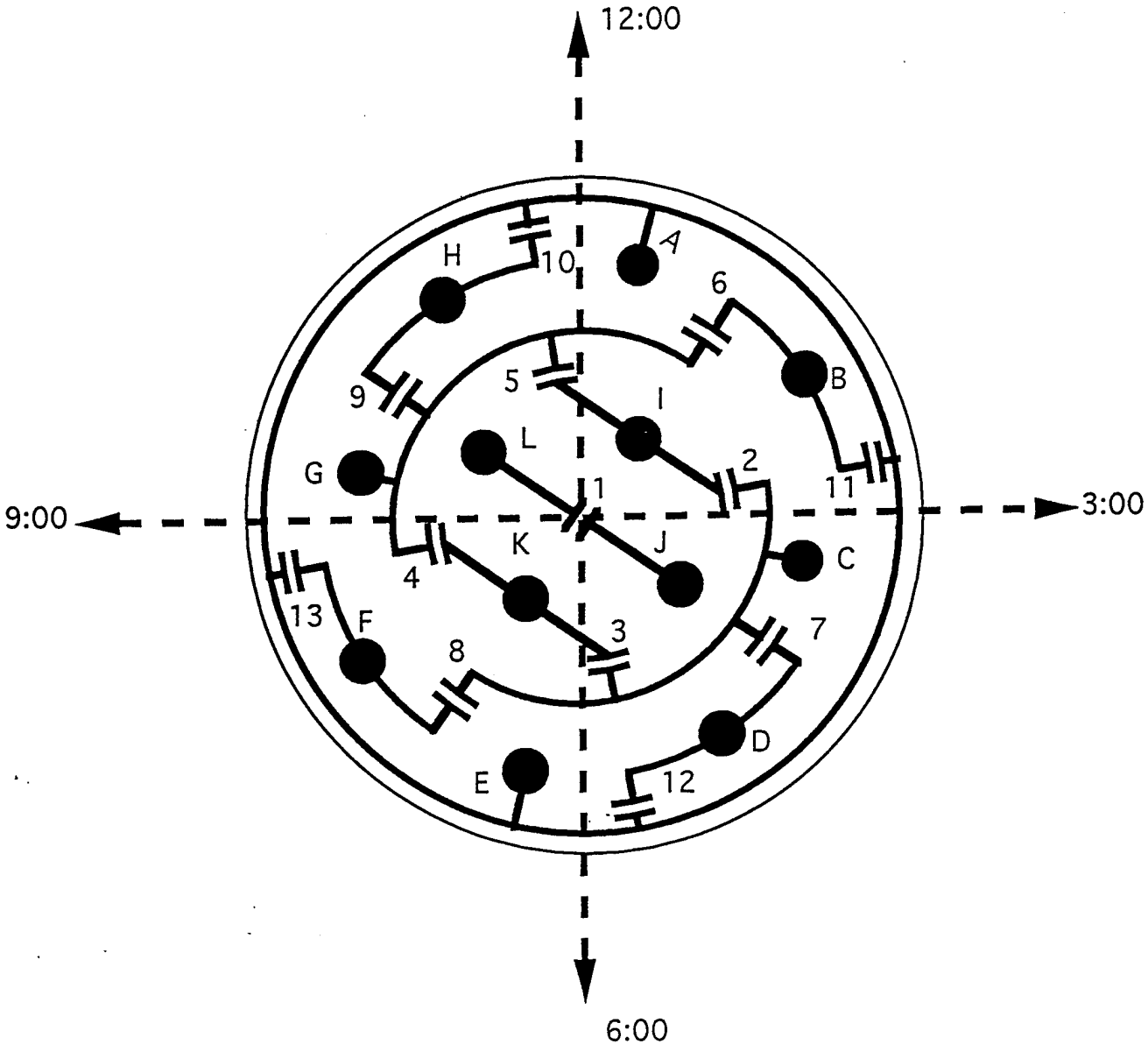

Figure 4: Configuration of wafer for surface temperature measurement. Ion implanted sensors are numbered 1-13. Connection pads are designated by letters A-L.

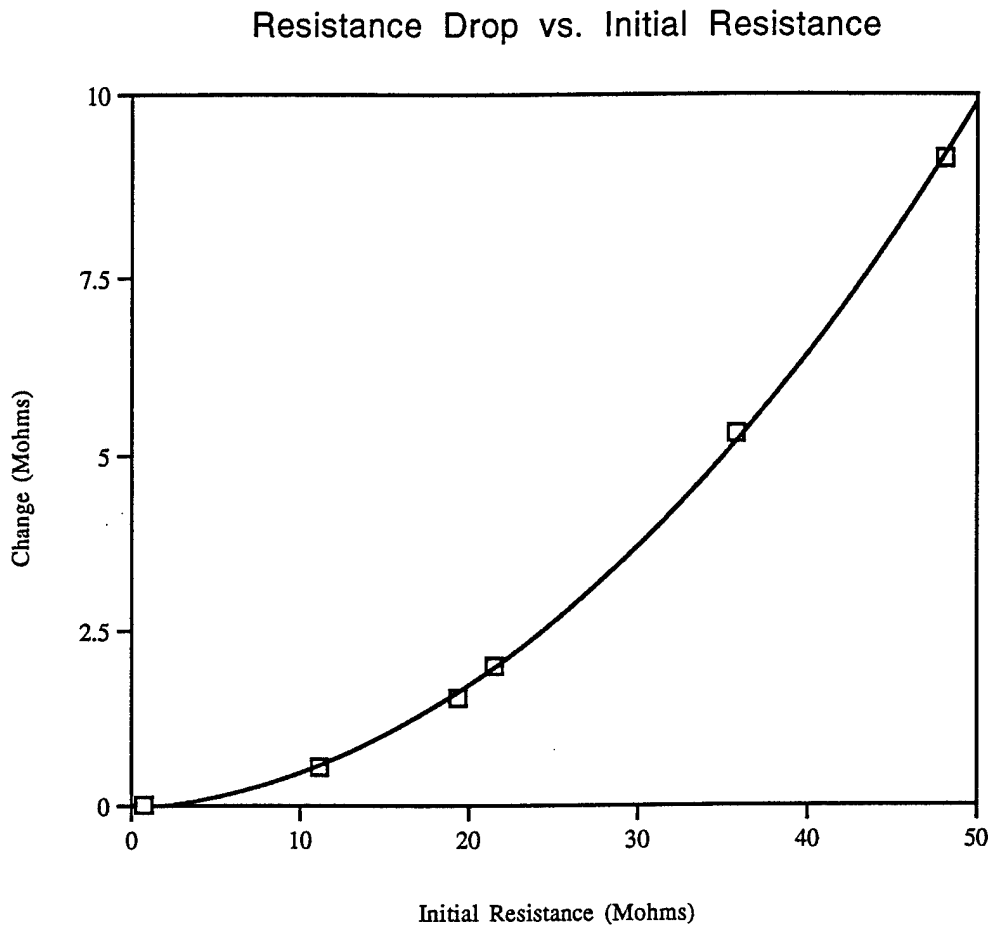

Figure 5: Drop in resistance on heating to 100°C versus sample resistance, various polymer types.

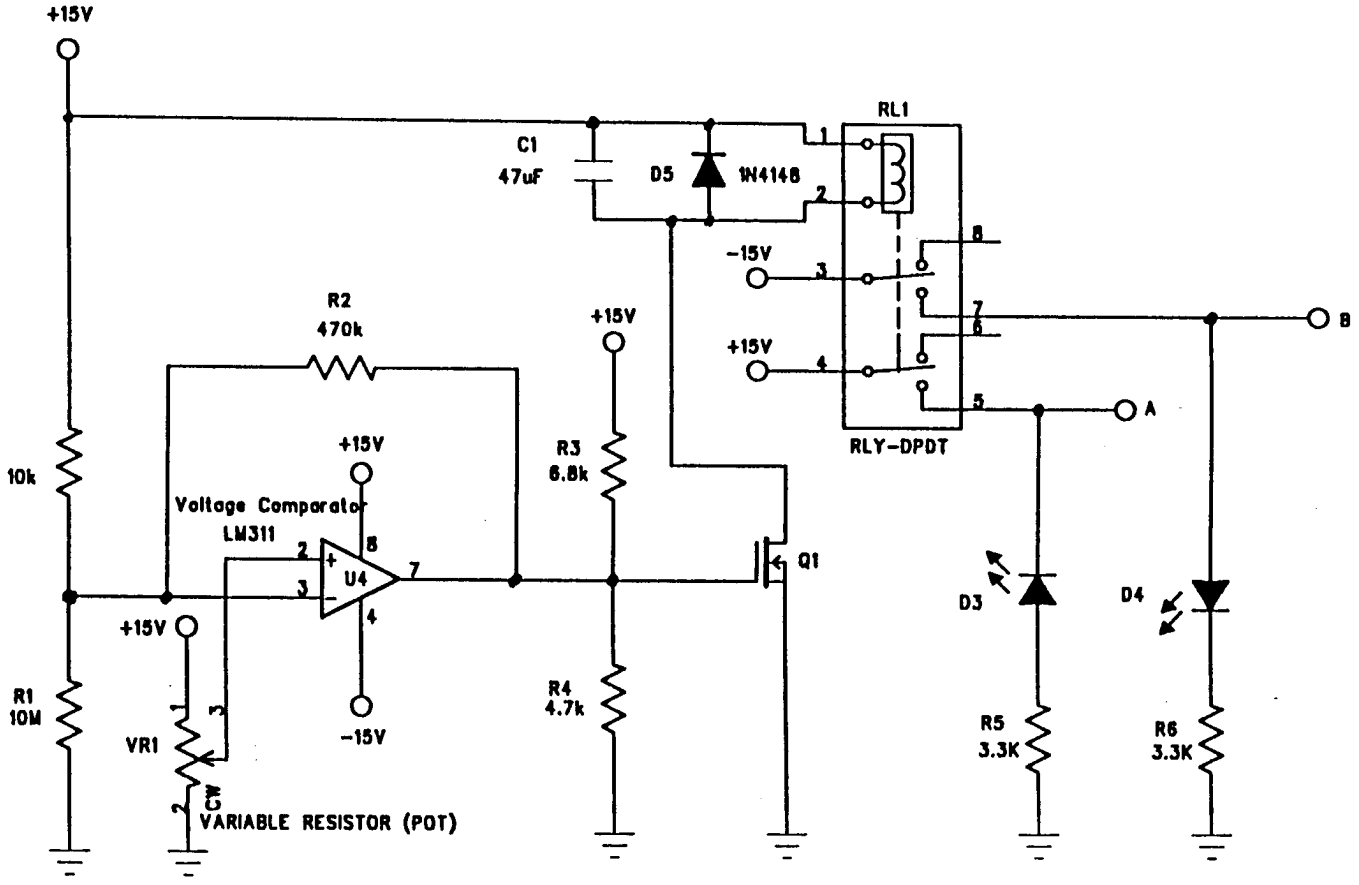

Figure 6a: Circuit for thermal overload protection using ion implanted thermistor. Components are described in text.

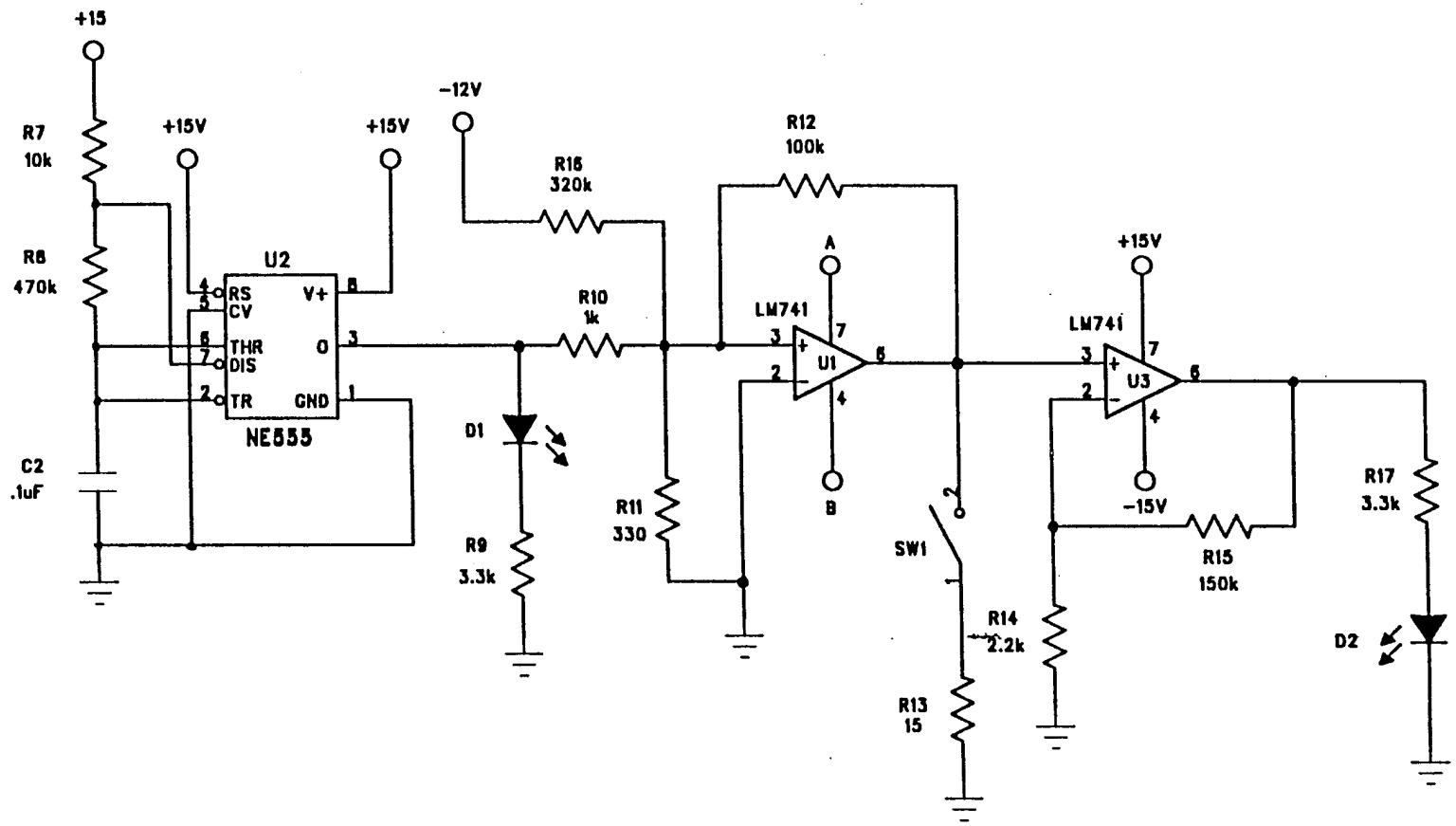

Figure 6b: Continuation of Figure 6a.